Explosive Detection Using a Novel Dielectric Barrier Discharge Ionisation Source for Mass Spectrometry

Author: Carl Fletcher

University of Liverpool Electrical Engineering and Electronics Brownlow Hill Liverpool

Merseyside United Kingdom L69 3GJ

Email Add:carlf@liverpool.ac.uk

http://orcid.org/0000-0003-3693-4342

Author: Richard Sleeman

Mass Spec Analytical Ltd MSA Filton Bristol United Kingdom

Email Add:s@msaltd.co.uk

Author: John Luke

Mass Spec Analytical Ltd MSA Filton Bristol United Kingdom

Email Add:John.Luke@msaltd.co.uk

Author: Peter Luke

Mass Spec Analytical Ltd MSA Filton Bristol United Kingdom

Email Add:peter.luke@msaltd.co.uk

Corresponding Author: James W Bradley

University of Liverpool Electrical Engineering & Electronics Liverpool Merseyside

United Kingdom

Email Add:J.W.Bradley@liverpool.ac.uk

Abstract

The detection of explosives is of great importance, as is the need for sensitive, reliable techniques that require little or no sample preparation and short run times for high throughput analysis. In this work, a novel ionisation source is presented based on a dielectric barrier discharge (DBD). This not only effects desorption and ionisation, but also forms an ionic wind, providing mass transportation of ions towards the mass spectrometer. Furthermore, the design incorporates two asymmetric alumina sheets, each containing three DBDs, so that a large surface area can be analysed. The DBD operates in ambient air, overcoming the limitation of other plasma based techniques which typically analyse smaller surface areas and require solvents or gases. A range of explosives across four different functional groups was analysed using the DBD with low limits of detection for cyclotrimethylene trinitramine (RDX) (100 pg), pentaerythritol trinitrate (PETN) (100 pg), hexamethylene triperoxide diamide(HMTD) (1 ng) and trinitrotoluene (TNT) (5 ng). Detection was achieved without any sample preparation or the addition of reagents to facilitate adduct formation.

Introduction

The detection of explosives is of crucial importance in applications such as forensic science[1–3], environmental monitoring[4,5], aviation security[6] and public safety[7]. Mass spectrometry is typically the technique of choice for forensic analysis as it offers great sensitivity, selectivity and speed. The ability to derive mass spectral information from samples within the ambient environment, ambient mass spectrometry, has attracted significant attention over the past decade. Many of these techniques require little or no sample preparation, and ionisation occurs external to the mass spectrometer. Desorption electrospray ionisation (DESI) was described in 2004, which utilises an electrospray, producing charged solvent ions which collide with the sample causing desorption/ionisation[8]. Following DESI came direct analysis in real time (DART) which ionises analytes by means of collisions with electronically excited species such as helium metastables[9].

Since the introduction of DART and DESI, ambient mass spectrometry (AMS) developed rapidly with many plasma based techniques such as low temperature plasma (LTP)[10], dielectric barrier discharge ionisation (DBDI)[11], plasma assisted desorption ionisation (PADI)[12], atmospheric pressure plasma jet (APPJ)[13], micro-plasma in a hollow cathode discharge (MCHD)[14], high-power pulsed microplasma jet (HPPMJ)[15], atmospheric pressure glow discharge (APGD)[16] and flowing atmospheric pressure afterglow (FAPA)[17]. The likes of DART and DESI enjoy greater advantages over other techniques, owing to the fact that they are commercially available and well described in the literature. The main limitations of all of these ambient ionisation sources are the use of expensive discharge gases such as helium, the use of environmentally harmful solvents and a small surface area for desorption/ionisation, typically less than 10 mm^2. Although some ionisation sources have been created with an array of plasma jets in an attempt to increase the surface area, disadvantages persist. For example, Dalgleish *et al.,* described an LTP probe consisting of 1, 7 and 19 individual jets[18], which increased the surface area for analysis, but also required a higher gas flow of helium. Furthermore, the surface area is still small, relative to a swab, for example. Within arrays of plasma DBD jets, there are strong repulsion forces which result in a divergence of the plasma plumes which may result in a non-uniform, non-reproducible

ionisation source for sample analysis[19]. Uniformity is important for routine screening analysis where, for example, a swab of a surface may be conducted; analysis of a small surface area would require several repeat analyses as the target analyte could be present on any part of that swab. The ability to analyse a larger surface area allows for the whole swab to be analysed in a single step, increasing throughput and confidence that the swab did or did not contain an analyte of interest. Furthermore, for explosive detection, an adduct of some form is usually formed with the explosive molecule, increasing identification confidence, and increasing sensitivity (detection probability). Routinely, for nitroesters such as pentaerythritol trinitrate (PETN) and nitroglycerin (NG) and nitroamines such as cyclotrimethylene trinitramine (RDX), a chloride ion is used to form an adduct with the explosive molecule to form the $[M+Cl]^-$ species[3].

In this paper a plasma ionisation source is described which operates in ambient air without the requirement for a gas flow or solvent, and has an analytical surface area of approximately 540 mm^2. The design of the DBD consists of two alumina sheets, each containing three pairs of electrodes. The pairs create surface DBD actuators by having ground electrodes on one side and powered electrodes on the reverse side of the alumina. The powered and ground electrodes overlap, but are not aligned. The misalignment of the powered and ground electrodes results in plasma actuation, an 'ionic wind' largely consisting of neutrals and gaseous ions, the latter of which are accelerated by the electric field[20,21]. The chordwise ionic wind travels in the direction of the ground electrodes and therefore, in this instance, towards the mass spectrometer, aiding ion transportation. Furthermore, the two alumina sheets are located opposite one another with the powered electrodes facing each other and separated by 4 mm. The plasma produces ozone, which reacts in ambient air to form NO_3^- ions[22]. These ions form adducts which can be exploited for explosive detection. The limits of detection achieved for four functional groups of explosives using a triple quadrupole mass spectrometer were; pentaerythritol tetranitrate PETN (100 pg) and cyclotrimethylenetrinitramine RDX (100 pg), hexamethylene triperoxide diamine (HMTD) (1 ng) and trinitrotoluene (TNT) (5 ng). The results presented were obtained without the addition of special gases (e.g. helium), solvents or adduct forming reagents (other than those naturally produced in the plasma).

Experimental

DBD Ion Source

The surface barrier discharge consisted of two alumina plates 91 x 79 x 0.5 mm (Ceramic Substrates & Components Ltd, Newport, Isle of Wight, UK). On each plate there are three powered electrodes and three ground electrodes, all of which are 60 mm long and 5 mm wide made up of adhesive copper tape. The three powered electrodes are on the same side of the alumina separated by a 7 mm gap and the ground electrodes are in the same configuration on the reverse side of the alumina. The ground and powered electrodes are slightly offset from one another but overlap by 1 mm (See Fig. 1 for schematic of the DBD). The offset electrodes result in the production of a chordwise ionic wind in the direction of the ground electrodes, with the plasma forming on the leading edge and extending a few mm. It can be seen in Fig.1 that the ground electrodes are closer to the mass spectrometer than the powered electrodes, and therefore, the ionic wind travels towards the mass spectrometer. The two DBD plates are identical to one another and are separated by 4 mm; however the powered electrodes on each DBD are positioned opposite each other creating a plasma actuator tunnel. The resulting tunnel is open at the front and sides and is 91 mm wide, 79 mm long with a gap

of 4 mm between each sheet. Finally, the powered electrodes remain exposed, whereas the ground electrodes are encapsulated in a dielectric material, Kapton tape in this case, to prevent a breakdown of plasma on the grounded surface. The flow generated by the resulting ionic wind has not been recorded but previous literature of a similar electrode configuration would suggest it to be 2 m/s[21]. Literature reports suggest that having additional actuators can increase the flow up to 10 m/s[23,24]. Other than the chordwise ionic wind, no special gases are added to effect ion transport.

A sinusoidal AC high voltage (6-8 kV, 20 kHz) was applied to the powered copper electrodes using a commercial audio amplifier (img Stage Line, STA-800) which was driven using a digital function generator (TG2000; AIM-TTI Instruments, Huntingdon, Cambridgeshire, UK). A custom built voltage step-up transformer (Express Transformers, Runcorn, UK) was connected to the output stage to enable high voltages required for gas breakdown. The peak to peak voltage was 7 kV and the voltage measurements were recorded using a high voltage probe (Pintek Electronics, HVP-15HF) and the frequency was fixed at 20 kHz. Voltage measurements were recorded using a Gould OS300 20 MHz dual trace oscilloscope (Gould, Ilford, Essex, UK). The current monitored was 20 mA using a Fluke 79 Series III multimeter (Fluke Europe B.V., Eindhoven, Netherlands). Schematic of DBD setup shown in Fig. 1. The operating temperature of the DBD is roughly 100 °C which allows for direct analysis from thermally labile surfaces such as polypropylene. The temperature was measured using a handheld infrared thermometer (Titan Power Tools (UK) Ltd, BA22 8RT) on the ground electrodes on the top of the alumina plate. Therefore, it is likely that the electrodes and resulting plasma inside are slightly above 100 °C, but is not efficient to result in damage to a polypropylene swab that has been subjected to the plasma for three seconds. The liberation of a sample from a polypropylene surface is not likely to be via thermal desorption, but through other mechanisms. It is possible that the oxygen and nitrogen and other excited species in the air, as a result of plasma interactions, are responsible for desorption through a transfer of their potential energy to the surface, similar to that with helium in PADI[25]. Salter *et al*., recently studied the effect of thermal desorption with PADI and suggest that while thermal desorption does contribute to the overall desorption in PADI, the main desorption process must be due to more complicated plasma mechanisms[26], which has been previous suggested to be excited species such as (He*) helium metastables[9].

Hiden HPR-60 Molecular Beam Mass Spectrometer

The DBD ion source was interfaced to an HPR-60 molecular beam mass spectrometer (MBMS) (Hiden Analytical Ltd, Warrington, UK) which utilises a single-stage quadrupole mass spectrometer (QMS). The MBMS is capable of sampling ions directly without the need for an internal ionisation source. The instrument can also sample radical and neutral species using an internal electron beam ionisation source. The MBMS was operated in ion detection mode (no internal ionisation source) and so any ions that were detected must have originated from the external DBD ion source. The MBMS samples species via a multistage differentially pumped skimmer inlet and transferred through the mass spectrometer with minimal interaction with other species and without wall collisions. The pressure reduction stages are separated by various skimmer cones which allows for a free-jet expansion from atmospheric pressure into the low pressure region resulting in a molecular beam[12,27]. The MBMS was coupled with the DBD ionisation where the chordwise ionic wind produced enough flow for the ions produced from species within the ambient air to be directed into the molecular beam for analysis. There was no APCI needle (or additional ionisation mechanisms) or sample flow. The front cone of the MBMS, due to the multistage differentially pumped inlet, is at

ambient pressure and does not create a significant amount of suction, which means the ion transportation mechanism responsible for ions entering the mass spectrometer was the ionic wind.

AB Sciex API 2000 Triple Quadrupole Mass Spectrometer

The DBD tunnel was connected to a custom built plenum chamber for an AB Sciex API 2000 triple quadrupole mass spectrometer (AB Sciex, Concord, Ontario, Canada), which also contained an in-line filter to capture dust and debris, as well as a ceramic transfer line to an atmospheric pressure chemical ionisation (APCI) corona discharge needle (as described previously [28,29]). The APCI needle is complimentary to the DBD and leads to an increase in sensitivity. The optimised global parameters for the mass spectrometer were: Curtain Gas (CUR): 10.0 psi, Collision-Induced Dissociation Gas (CID/CAD): 3 V, Nebuliser Current (NC): -6.0 µA, Q1 resolution (ion energy): -1.0 V, Q3 resolution (ion energy): -2.7 V, Deflector: 50.0 V and a sample pump was utilised to draw ions towards the mass spectrometer with a flow of approximately 21 L/min. Although ions are detected without this additional sample flow (provided no plenum chamber is used, thus reducing the distance the ions have to travel), it was found that the sample flow increased the sensitivity by improving ion transportation in the direction of the mass spectrometer orifice. The sample flow also acts as a cooling system to maintain the temperature of the DBD. Unit mass resolution was used. (Where values are given as a negative value the mass spectrometer was in negative ion mode, and vice versa).

Sciex X500R QTOF Mass Spectrometer

In addition to the AB Sciex API 2000, a Sciex X500R QTOF instrument was also used during this study for accurate mass measurements (AB Sciex, Concord, Ontario, Canada). This instrument used the following conditions: Firmware: ATLAS_QTOF_ICX_v0 03 (0 03), Software: SCIEX OS 1.2, Scan type: SWATH (sequential windowed acquisition of all theoretical masses), Polarity: negative, Ionspray (v): -4300 V, CAD gas: 7 V, TOFMS start mass: 100 (Da), TOFMS stop mass: 500 (Da), Accumulation time: 0.05 (s), Declustering potential (DP): -20 V, DP spread: 0 V, Collision energy (CE): -5 V, CE spread: 0. For TOFMSMS the parameters used were: Start mass: 30 (Da), Stop mass: 500 (Da), Accumulation time: 0.03 (s), Rolling CE: False, Charge state: 1, DP: -10 V, DP Spread: 0, CE: -30 V, CE spread: 15 V.

Sample Preparation

The samples used for this study were obtained from Kinesis Ltd (Kinesis Ltd, St. Neots, Cambridgeshire, UK) and contained TNT 1 mL 1000 µg/mL in MeOH:AcCN (1:1), RDX 1 mL 1000 µg/mL in MeOH:AcCN, PETN 1 mL 1000 µg/mL in MeOH and HMTD 1 mL 100 µg/mL in AcCN which were all subsequently diluted using methanol (> 95% HPLC grade) from Charlton Scientific (Charlton Scientific Ltd, Charlton, Oxon, OX17 3DR, UK). For analysis, the samples were spotted onto a glass slide, left to dry, and then swabbed with polypropylene (Rayoface C50) (Innovia, Wigton, Cumbria, UK) before being placed directly in the plasma for 2-3 seconds for liberation/ionisation. Where 'real-world' samples are referenced, these consist of samples from a real explosive composition of Semtex 1H provided by a UK government stakeholder, the further prevalence of the composition is unknown. These samples were collected by handling a heavily contaminated mobile phone, wearing gloves, before depositing the sample in a series of fingerprint depositions.

Results & Discussion

DBD Ion Source with Molecular Beam Mass Spectrometry

The objectives of this study were twofold; to establish the effectiveness of the DBD as an ionisation source and to quantify how significant the ionic wind was in terms of successful ion transportation. The DBD ion source was integrated with a MBMS by aligning the bottom DBD sheet to be roughly 1 mm below the orifice to the mass spectrometer. As the DBD operates in ambient air, it was anticipated that enough reactive species would be present to demonstrate ion production. As the DBD produces its own ionic wind, no additional gas flows would be required. The MBMS was operated in both positive and negative ion modes between m/z 0 and 200. Five repeats of each cycle were taken and averaged to produce the mass spectral data displayed in Fig. 2. The negative ion data can be seen in Fig. 2.a. where the two most dominant peaks are at m/z 62 (presumed to be NO_3^-), and m/z 125 (presumed to be $[HNO_3(NO_3)]^-$). The positive ion data in Fig 2.b. shows that the most dominant peaks are formed from (presumed) water clusters at m/z 55, 73, 91 and 109 for $[H_3O(H_2O)_n]^+$, where n = 2, 3, 4 and 5 respectively.

The data produced by coupling the DBD to an MBMS proved that the DBD is capable of operating in ambient air without additional gas flows and produces ions in both positive and negative ion modes. Furthermore, the DBD creates its own chordwise ionic wind which provides ion transportation in the direction of the mass spectrometer. However, it is unknown how efficient the ionic wind is for ion transportation as it is assumed that even if the induced flow is directed in the downstream direction (towards the ground electrode) that there must be some upstream flow too, caused by the ion motions within both half cycles of the sine applied voltage, which could lead to a reduction in efficiency[24].

DBD Ion Source with AB Sciex API 2000 Mass Spectrometer

Solutions were diluted to a workable concentration for optimisation (TNT, PETN and RDX 100 ng/µl in MeOH and HMTD 50 ng/µL in MeOH) and then infused using a syringe driver at 0.60 mL/hr through a glass capillary. The end of the capillary was placed 1 mm in front of the powered electrode nearest to the orifice. The plasma was then used to volatilise and ionise the sample before the ions formed were entrained in the air flow through a ceramic transfer line to an APCI needle. Although it is clear that ions are formed in the DBD without the need for the APCI needle, it is thought that clustering may occur during ion transport from the source to the orifice, and that the APCI needle helps to break these clusters, leading to a significant improvement in sensitivity. The post-ionisation of APCI offers the prospect of remote sampling, adding versatility to the DBD ion source by potentially making it possible to desorb, ionise and collect analyte ions from a sample and transfer them to the APCI needle and mass spectrometer through a tube, similar to the mechanism provided by other techniques[30,31].

This proposed mechanism was corroborated by using another custom built front end for the mass spectrometer which did not have a plenum chamber or APCI needle. This study demonstrated that the DBD does produce analyte ions, but the intensity was significantly reduced. This demonstrates that the ions were generated in the plasma, as opposed to the plasma liberating them from the surface (or volatilising a liquid sample) before being ionised by APCI. In APCI, the ions formed are different from those observed in these experiments. The results also demonstrate that the ions produced do not arise from an aspirator effect caused by high flows, as the DBD liberates and ionises samples without an APCI needle. It is

anticipated that further improvements in the design of the DBD source, such as the use of different shaped electrodes to focus the ions, and modification of the plenum chamber to reduce the distance ions have to travel, are likely to result in higher sensitivity. The plenum chamber is at ambient temperature but does increase, likely with heat transfer from the DBD; the ceramic transfer line is also not heated. Heating the plenum, transfer line, or both, may decrease condensation of explosives species on unheated surfaces, and this would be expected to lead to an increase in sensitivity. These possibilities are yet to be explored.

For TNT, the most dominant precursor ion observed was $[M-NO+HNO_3]^-$ at m/z 260, and whilst the deprotonated molecular ion $[M-H]^-$ at m/z 226 was also observed, the signal intensity was significantly lower than $[M-NO+HNO_3]^-$ at m/z 260. Therefore, this latter precursor ion was chosen. This observation is different from APCI, where the two most dominants ions are $[M]^-$ and $[M-H]^-$ at m/z 227 and 226[3], although, in examples where the ionisation happens in open air, the precursor ion $[M-NO+HNO_3]^-$ at m/z 260 is common[11,32,33]. The product ions of m/z 260 were the usual characteristic ions for TNT, $[M-NO]^-$ at m/z 197 and NO_2^- at m/z 46 , as shown in Fig. 3.a. For RDX the precursor ion detected was $[M+NO_3]^-$ at m/z 284, resulting in product ions at m/z 62 and 46 for NO_3^- and NO_2^- respectively, as depicted in Fig. 3.b. The adducted precursor ion for PETN was detected for both $[M+NO_3]^-$ at m/z 378 and $[M-NO_2+HNO_3]^-$ at m/z 333. As a 3-ion criterion is recommended for the reliable identification of a molecule using tandem mass spectrometry[34], both precursor ions were monitored, as they each produce a strong NO_3^- product ion at m/z 62, Fig. 3.c and d. respectively. The molecular ion for HMTD was observed in positive ion mode in the form of the protonated molecule ion $[M+H]^+$ at m/z 209. The two most dominant products for HMTD were observed at m/z 145 for $[M-CH_4O_3]^+$ (due to a loss of formaldehyde and hydrogen peroxide) and at m/z 88 for $[C_2H_6O_2N]^{+}$[35].

Whilst some of these products are observed in APCI, such as NO_3^- and NO_2^- at m/z 62 and 46 for nitro-containing explosives, and the $[M-CH_3O_3]^+$ ion at m/z 145 for HMTD, the dominance of the NO_3^- ion at m/z 62 is seldom seen in APCI. Furthermore, the product at m/z 88 for HMTD is also less commonly documented, largely because other higher mass products, such as $[M-CHO]^+$ and $[M-CH_3O_3]^+$ at m/z 179 and 145 respectively, are more dominant in the APCI mass spectrum. Ordinarily, explosive detection of nitrogen containing compounds using APCI makes use of adducts such as chlorine to enhance detection, because not only do they provide their own product ions for adducts incorporating $^{35}Cl^-$ and $^{37}Cl^-$ at m/z 35 and 37[3], but their isotopic patterns are very characteristic and can add another level of confidence for detection[36]. This evidence suggests a different ionisation mechanism to APCI which produces results similar to those presented in the literature[11,37]. Unlike in APCI, using plasma in air results in an abundance of ozone, which in turn is responsible for the reduction in the proton abstraction reaction, suggesting a possible reason why, in the case of TNT, the $[M-H]^-$ ion is not the most abundant[32,33].

Limits of detection for each functional group of explosive were ascertained by spotting a known concentration of solution onto a glass slide before allowing the solvent to evaporate. Once it was dry, the slide was swabbed firmly with a polypropylene strip which was placed directly in the plasma for 2-3 seconds for analysis. The limit of detection data are shown in Fig. 4 for TNT, RDX, PETN and HMTD. It can be seen in Fig. 4 that the LODs for RDX and PETN could be lower than 100 pg, but this limit is set at both ion pairs being above 3.5 x S/N ratio.

Polypropylene was used as the swabbing medium because it has a smooth surface and therefore, liberation of the sample should occur in a much shorter time than from for

example, textile surfaces. The use of polypropylene resulted in much higher signal intensities than PTFE, cotton paper or shark paper swabs. The limits of detection for RDX (100 pg), PETN (100 pg), HMTD (1 ng) and TNT (5 ng) should be viewed in the context that these samples were introduced after a secondary transfer step. In an operational context, it may be beneficial to use other swabbing media such as a textile based swab because the collection efficiency is likely to reflect the make-up of the matrix (pores and fibres etc.), and the desorption rate is slightly less efficient in comparison to a smooth surface such as polypropylene. While for most forensic applications this would be viewed as a disadvantage; it could be advantageous as more of the sample will remain on the swab after the first analysis and the swab could therefore be subjected to subsequent analyses. A fibre swab could allow for more than one technique to detect and identify the sample, however, this would be at a compromise to sensitivity.

In order to replicate surfaces which may be encountered in an operational context, a blind study consisting of four test boards, each containing a door handle, a plastic light switch and a melamine board were constructed. Figure 5 shows the results from a blind study where a contaminated gloved finger placed the 10th, 11th and 12th fingerprint of a real-world explosive onto one door handle, one plastic light switch and one melamine board respectively, leaving the other surfaces blank to measure any cross-contamination and interferences. The data in figure 5 was obtained using a polypropylene swab, note that the peaks are very short in time and high in intensity suggesting rapid desorption (unlike those shown in Fig. 6 with textile based swabs) and demonstrated the DBD ion source to be self-purging. This study aimed to reflect a real-world scenario of contamination using a real manufactured explosive as opposed to a certified reference standard and therefore, the sample was not 'clean' and contained a mixture of dyes, taggants, plasticisers and other compounds.

Only one substrate on each test board displayed contamination, the other test boards were correctly identified as being blank. This is important for forensic and detection applications, since false positives are expensive and time-consuming. Figure 5 also shows the contaminated surfaces analysed using a polypropylene swab and Fig. 6 shows the same surfaces re-analysed using Teflon coated fibreglass and Nomex swabs. All demonstrate detection of the target analytes even after the 4th transfer (deposit and 3 swabs). This brief study demonstrated the DBDs ability to detect explosives from an array of swabbing materials and surface types, demonstrating its versatility as an ionisation source for the mass spectrometric detection of explosives.

DBD Ion Source with Sciex X500R QTOF Mass Spectrometer

Figure 7 is from a sequential windowed acquisition of all theoretical fragment mass spectra (SWATH). A SWATH acquisition is an expanded mass isolation window which is stepped across the whole mass range of interest, and a composite MS/MS spectrum of all precursor masses from each mass window is obtained during each mass step. The sample shown in Fig. 7 was a swab of a glass slide that had been contaminated by a gloved finger than had touched a phone heavily contaminated with Semtex. This data shows the exact mass for PETN [M+NO$_3$]$^-$ at m/z 378.0099, and the formula finder in Fig. 7 has identified the formula C$_5$H$_9$N$_5$O$_{15}$ with an exact mass of m/z 378.0022, suggesting a 20.3 ppm calibration shift. Note that mass calibration was not performed directly before this analysis and therefore, a calibration shift is to be expected. These results are intended to show proof of principle and demonstrate the successful integration of the DBD ion source with a Sciex X500R QTOF instrument. A background peak known to be [HNO$_3$(NO$_3$)]$^-$ was subsequently used as a calibration peak, which has a known exact mass of m/z 124.9840. This was found at m/z

124.9870, suggesting a shift of 23.9 ppm. Taking this into account, the Semtex data was within 5 ppm (See figure S. 1 in supporting information). Finally, Fig. 7 also shows the exact mass for RDX [M+NO$_3$]$^-$ at *m/z* 284.0294. The formula finder suggests a formula of C$_3$H$_7$N$_7$O$_9$, with an exact mass of 284.0232, suggesting a calibration shift of 21.7 ppm. The MS/MS data has not been presented here, but both spectra show products at *m/z* 46 and 62 for NO$_2^-$ and NO$_3^-$, as expected.

LODs have not been ascertained on the X500R QTOF yet, but it is assumed that the LOD will be improved. Firstly, the QTOF is more advanced than the API 2000 triple quadrupole and should be capable of higher sensitivities. Further the LOD data obtained on the API 2000 in Fig. 4 shows that the limit of detection for the NO$_3^-$ product ion at *m/z* 62 could be much lower than 100 pg as the peak is much larger the 3.5 x S/N ratio. However, due to the abundance of additional information that can be obtained with the X500R QTOF, such as accurate mass, there is a higher degree in confidence and therefore, the second ion pair may not be necessary for identification, circumventing the need for the 3-ion criterion and allowing for improved LODs.

Conclusion

This paper describes a DBD plasma ionisation source capable of being coupled to many types of mass spectrometer (and potentially other types of instrument) for the rapid screening of explosives. It enjoys high sensitivity, reproducibility and selectivity in a real world context and using various swabbing materials. The DBD plasma source is able to identify explosives without the use of chromatography, solvents or the formation of adducts. The DBD has the ability to ionise in both positive and negative ion modes for small molecule analysis, and therefore could be deployed for many other analytical applications such as the detection of substances of abuse. Finally, the DBD ion source has the potential to be made field portable, and reduces consumable costs and harm to the environment.

Acknowledgements

References

[1]   X. Xu, M. Koeberg, C.-J. Kuijpers, E. Kok. Development and validation of highly selective screening and confirmatory methods for the qualitative forensic analysis of organic explosive compounds with high performance liquid chromatography coupled with (photodiode array and) LTQ ion trap/Orbitrap mass spectrometric detection(HPLC-(PDA)-LTQOrbitrap. *Sci. Justice* **2014**, *54*, 3.

[2]   L. T. Demoranville, T. M. Brewer. Ambient pressure thermal desorption ionization mass spectrometry for the analysis of substances of forensic interest. *Analyst* **2013**, *138*, 5332.

[3]   C. S. Evans, R. Sleeman, J. Luke, B. J. Keely. A rapid and efficient mass spectrometric method for the analysis of explosives. *Rapid Commun. Mass Spectrom.* **2002**, *16*, 1883.

[4]   C. A. Crowson, H. E. Cullum, R. W. Hiley, A. M. Lowe. A Survey of High Explosives Traces in Public Places. **1996**, *41*, 980.

[5]   H. E. Cullum, C. Mcgavigan, C. Z. Uttley, M. A. M. Stroud, D. C. Warren. A Second Survey of High Explosives Traces in Public Places ∗. **2004**, *49*, 1.

[6]   S. Singh, M. Singh. Explosives detection systems (EDS) for aviation security. *Signal Processing* **2003**, *83*, 31.

[7]   I. Cotte-Rodríguez, R. G. Cooks. Non-proximate detection of explosives and chemical warfare agent simulants by desorption electrospray ionization mass spectrometry. *Chem. Commun.* **2006**, *0*, 2968.

[8]   Z. Takáts, J. M. Wiseman, B. Gologan, R. G. Cooks. Mass spectrometry sampling under ambient conditions with desorption electrospray ionization. *Science* **2004**, *306*, 471.

[9]   R. B. Cody, J. A. Laramée, H. D. Durst. Versatile new ion source for the analysis of materials in open air under ambient conditions. *Anal. Chem.* **2005**, *77*, 2297.

[10]   J. D. Harper, N. A. Charipar, C. C. Mulligan, X. Zhang, R. G. Cooks, Z. Ouyang. Low-temperature plasma probe for ambient desorption ionization. *Anal. Chem.* **2008**, *80*, 9097.

[11]   N. Na, C. Zhang, M. Zhao, S. Zhang, C. Yang, X. Fang, X. Zhang. Direct detection of explosives on solid surfaces by mass spectrometry with an ambient ion source based on dielectric barrier discharge. *J. Mass Spectrom.* **2007**, *42*, 1079.

[12]   L. V Ratcliffe, F. J. M. Rutten, D. A. Barrett, T. Whitmore, D. Seymour, C. Greenwood, Y. Aranda-Gonzalvo, S. Robinson, M. McCoustra. Surface analysis under ambient conditions using plasma-assisted desorption/ionization mass spectrometry. *Anal. Chem.* **2007**, *79*, 6094.

[13]   E. Stoffels, A. J. Flikweert, W. W. Stoffels, G. M. W. Kroesen. Plasma needle: a non-destructive atmospheric plasma source for fine surface treatment of (bio)materials. *Plasma Sources Sci. Technol.* **2002**, *11*, 383.

[14]   J. M. Symonds, A. S. Galhena, F. M. Fernández, T. M. Orlando. Microplasma discharge ionization source for ambient mass spectrometry. *Anal. Chem.* **2010**, *82*, 621.

[15]   T. Iwai, K. Kakegawa, K. Okumura, M. Kanamori-Kataoka, H. Miyahara, Y. Seto, A. Okino. Fundamental properties of a touchable high-power pulsed microplasma jet and its application as a desorption/ionization source for ambient mass spectrometry. *J. Mass Spectrom.* **2014**, *49*, 522.

[16]   J. T. Shelley, S. J. Ray, G. M. Hieftje. Laser ablation coupled to a flowing atmospheric pressure afterglow for ambient mass spectral imaging. *Anal. Chem.* **2008**, *80*, 8308.

[17]   F. J. Andrade, J. T. Shelley, W. C. Wetzel, M. R. Webb, G. Gamez, S. J. Ray, G. M. Hieftje.

Atmospheric pressure chemical ionization source. 1. Ionization of compounds in the gas phase. *Anal. Chem.* **2008**, *80*, 2646.

[18]   J. K. Dalgleish, M. Wleklinski, J. T. Shelley, C. C. Mulligan, Z. Ouyang, R. Graham Cooks. Arrays of low-temperature plasma probes for ambient ionization mass spectrometry. *Rapid Commun. Mass Spectrom.* **2013**, *27*, 135.

[19]   M. Ghasemi, P. Olszewski, J. W. Bradley, J. L. Walsh. Interaction of multiple plasma plumes in an atmospheric pressure plasma jet array. *J. Phys. D. Appl. Phys.* **2013**, *46*, 52001.

[20]   M. Robinson. A History of the Electric Wind. *Am. J. Phys.* **1962**, *30*, 366.

[21]   R. Erfani, H. Zare-Behtash, C. Hale, K. Kontis. Development of DBD plasma actuators: The double encapsulated electrode. *Acta Astronaut.* **2015**, *109*, 132.

[22]   K. Sekimoto, M. Takayama. Negative ion formation and evolution in atmospheric pressure corona discharges between point-to-plane electrodes with arbitrary needle angle. *Eur. Phys. J. D* **2010**, *60*, 589.

[23]   F. O. Thomas, T. C. Corke, M. Iqbal, A. Kozlov, D. Schatzman. Optimization of Dielectric Barrier Discharge Plasma Actuators for Active Aerodynamic Flow Control. *AIAA J.* **2009**, *47*, 2169.

[24]   M. Forte, J. Jolibois, J. Pons, E. Moreau, G. Touchard, M. Cazalens. Optimization of a dielectric barrier discharge actuator by stationary and non-stationary measurements of the induced flow velocity: Application to airflow control. *Exp. Fluids* **2007**, *43*, 917.

[25]   J. T. Shelley, J. S. Wiley, G. C. Y. Chan, G. D. Schilling, S. J. Ray, G. M. Hieftje. Characterization of direct-current atmospheric-pressure discharges useful for ambient desorption/ionization mass spectrometry. *J. Am. Soc. Mass Spectrom.* **2009**, *20*, 837.

[26]   T. L. Salter, I. S. Gilmore, A. Bowfield, O. T. Olabanji, J. W. Bradley. Ambient Surface Mass Spectrometry Using Plasma-Assisted Desorption Ionization: Effects and Optimization of Analytical Parameters for Signal Intensities of Molecules and Polymers. *Anal. Chem.* **2013**, *85*, 1675.

[27]   B. Davide, U. Buck, in *Atomic and Molecular Beam Methods*, (Ed: G. Scoles). Oxford University Press, New York, **1988**, pp. 499–524.

[28]   K. A. Ebejer, R. G. Brereton, J. F. Carter, S. L. Ollerton, R. Sleeman. Rapid comparison of diacetylmorphine on banknotes by tandem mass spectrometry. *Rapid Commun. Mass Spectrom.* **2005**, *19*, 2137.

[29]   C. M. Fletcher, R. Sleeman. Rapid identification of seized controlled substances and related compounds by tandem mass spectrometry without chromatography. *Rapid Commun. Mass Spectrom.* **2016**, *30*, 908.

[30]   J. Balog, L. Sasi-Szabo, J. Kinross, M. R. Lewis, L. J. Muirhead, K. Veselkov, R. Mirnezami, B. Dezso, L. Damjanovich, A. Darzi, J. K. Nicholson, Z. Takats. Intraoperative Tissue Identification Using Rapid Evaporative Ionization Mass Spectrometry. *Sci. Transl. Med.* **2013**, *5*, 194ra93.

[31]   J. Balog, S. Kumar, J. Alexander, O. Golf, J. Huang, T. Wiggins, N. Abbassi-Ghadi, A. Enyedi, S. Kacska, J. Kinross, G. B. Hanna, J. K. Nicholson, Z. Takats. In Vivo Endoscopic Tissue Identification by Rapid Evaporative Ionization Mass Spectrometry (REIMS). *Angew. Chemie Int. Ed.* **2015**, *54*, 11059.

[32]   D. T. Usmanov, L. C. Chen, Z. Yu, S. Yamabe, S. Sakaki, K. Hiraoka. Atmospheric pressure chemical ionization of explosives using alternating current corona discharge ion source. *J. Mass Spectrom.* **2015**, *50*, 651.

[33]   D. T. Usmanov, Z. Yu, L. C. Chen, K. Hiraoka, S. Yamabe. Low-pressure barrier discharge ion source using air as a carrier gas and its application to the analysis of drugs and explosives. *J. Mass Spectrom.* **2016**, *51*, 132.

[34]   J. A. Sphon. Use of mass spectrometry for confirmation of animal drug residues. *J. Assoc. Off. Anal. Chem.* **1978**, *61*, 1247.

[35]   A. J. Peña-Quevedo, S. P. Hernández-Rivera. Mass spectrometry analysis of hexamethylene triperoxide diamine by its decomposition products. **2009**, *7303*, 730303.

[36]   I. A. Popov, H. Chen, O. N. Kharybin, E. N. Nikolaev, R. G. Cooks. Detection of explosives on solid surfaces by thermal desorption and ambient ion/molecule reactions. *Chem. Commun.* **2005**, *2*, 1953.

[37]   J. K. Dalgleish, K. Hou, Z. Ouyang, R. G. Cooks. In Situ Explosive Detection Using a Miniature Plasma Ion Source and a Portable Mass Spectrometer. *Anal. Lett.* **2012**, *45*, 1440.
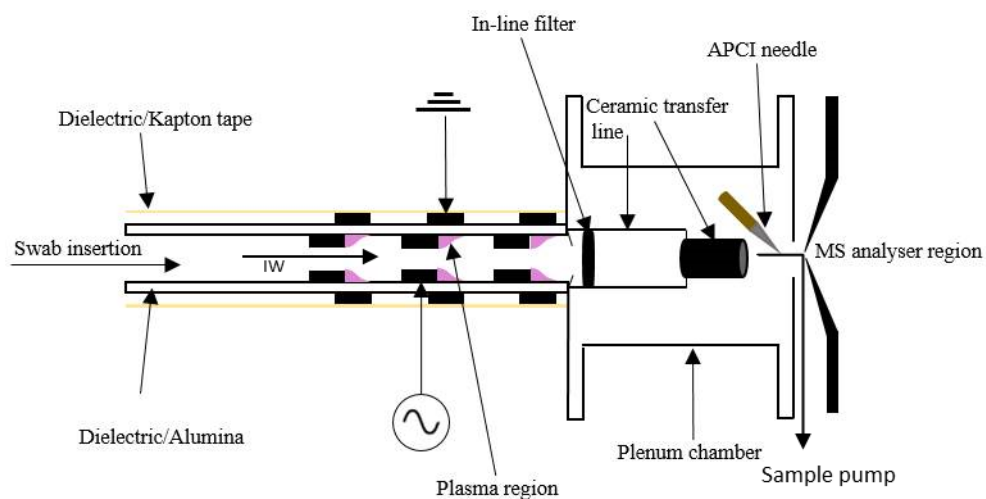
Figure 1: Schematic of DBD ion source coupled with plenum chamber and APCI needle. The ionic wind produced is represented by 'IW'.
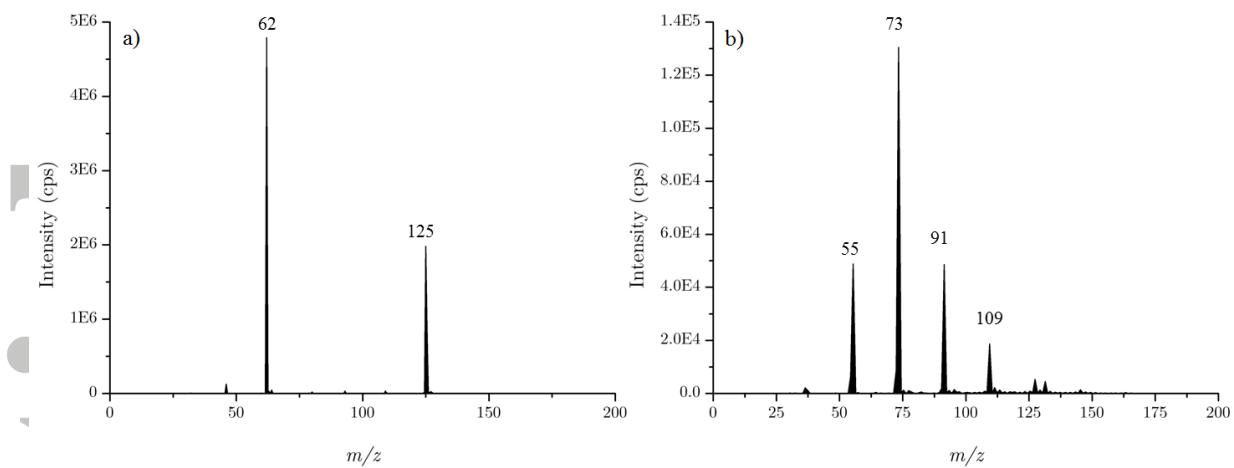
Figure 2: MBMS spectra of the DBD ion source operated in (a) negative ion mode, and (b) positive ion mode.

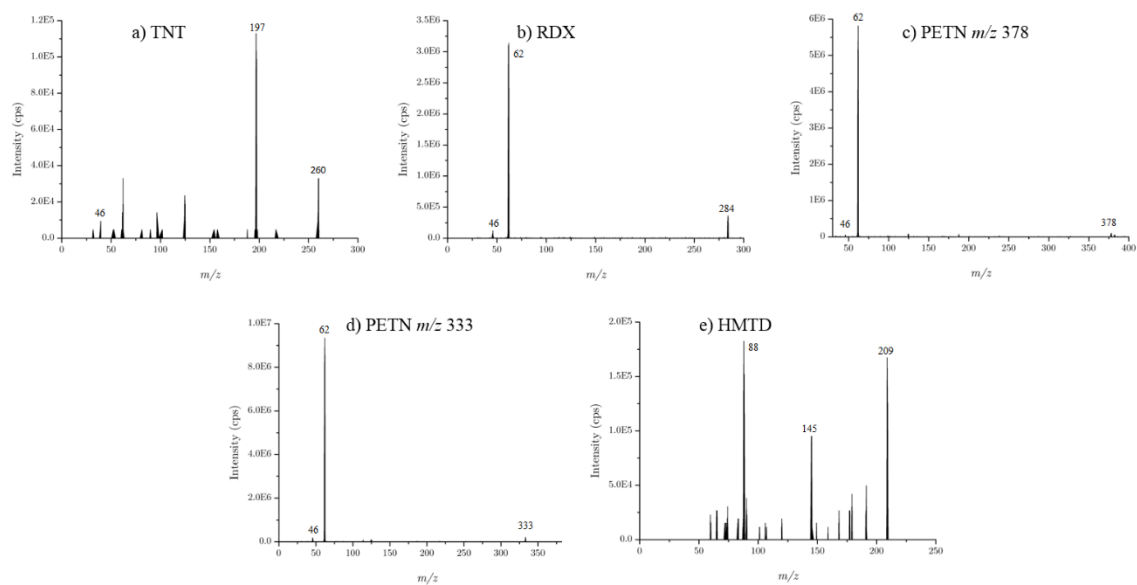Figure 3: MS/MS mass spectra of explosives infused by capillary for a) TNT (100 ng/µL), b) RDX (100 ng/µL), c) PETN (100 ng/µL) products of m/z 378, d) PETN (100 ng/µL) products of m/z 333 and e) HMTD (50 ng/µL).
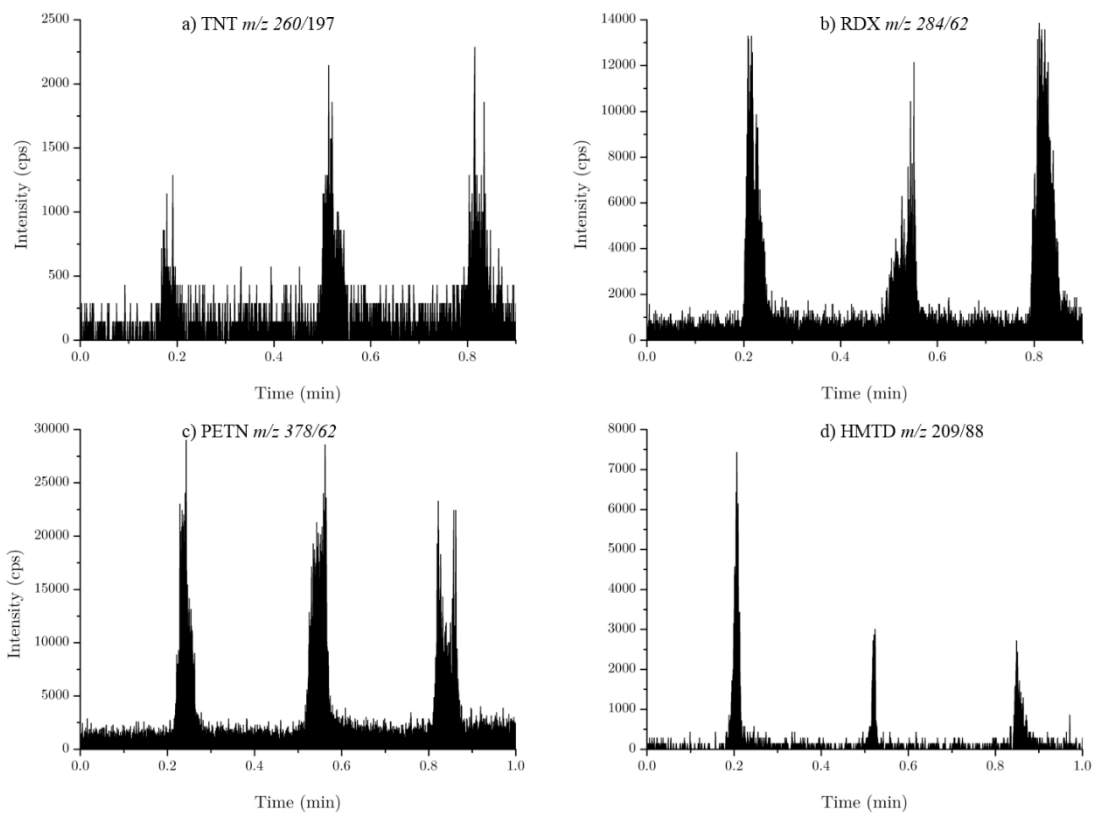
Figure 4: MRM mass spectra of the limits of detection using polypropylene swabs of samples spotted onto a glass slide for a) 5 ng/μL TNT m/z 260/197, b) 100 pg/μL RDX m/z 284/62, c) 100 pg/μL PETN m/z 378/62 and d) 1 ng/μL HMTD m/z 209/88.
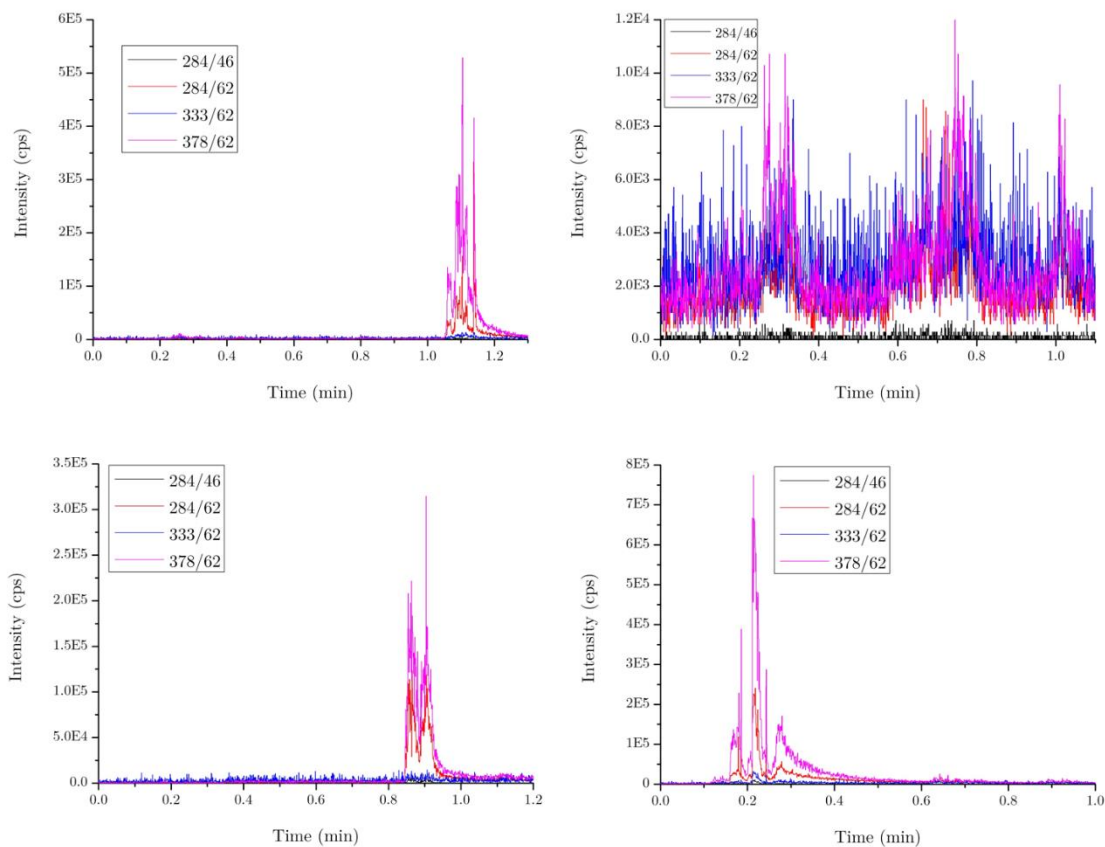
Figure 5: All multiple reaction monitoring (MRM) spectra for RDX and PETN taken from a blind study of Semtex deposited on various surfaces. All spectra show 3 swabs from 3 different surfaces in the order: Handle, light switch, melamine board, taken with polypropylene swabs. Top left shows PETN and RDX detected on the melamine board, top right shows all 3 surfaces are blank, bottom left shows contamination on the light switch and bottom right shows contamination on the handle. All other surfaces correctly identified as being blank.
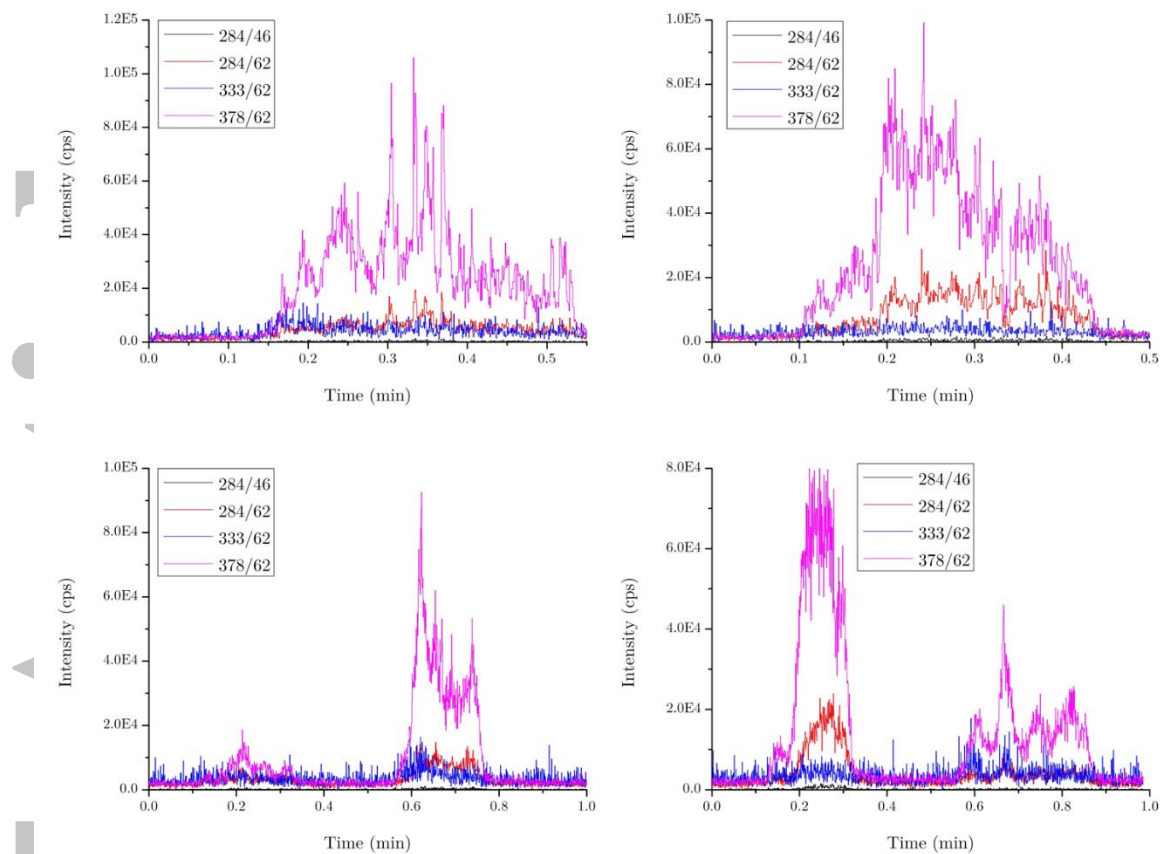
Figure 6: MRM mass spectra of the same surfaces being re-analysed using different swabbing materials. Top left is a Teflon coated fibreglass (TCFG) swab on the melamine board, top right is a Nomex swab of the melamine board, bottom left is TCFG and Nomex swabs of the light switch and bottom right is TCFG and Nomex swabs of the handle.
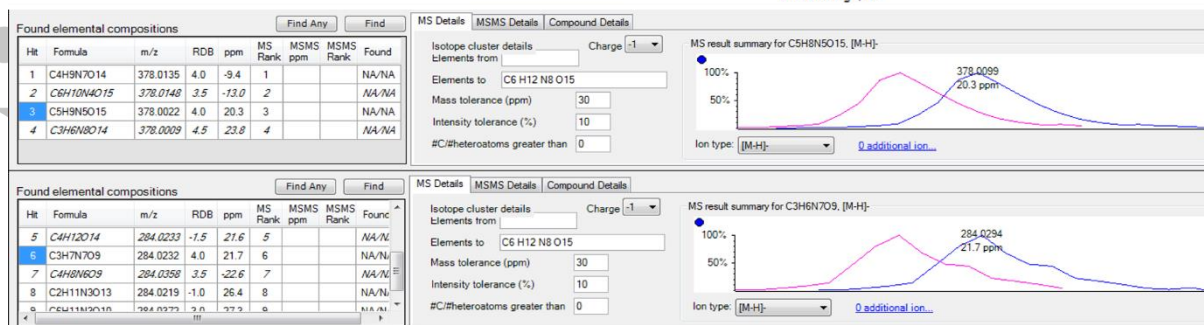
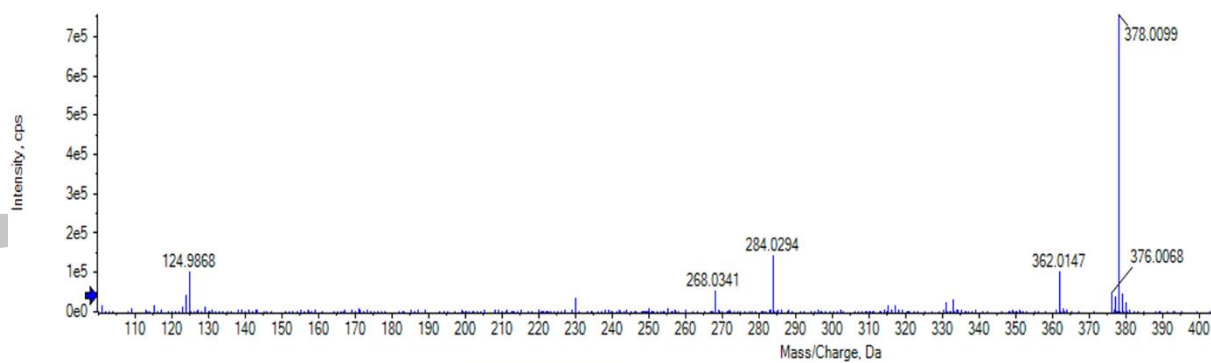Figure 7: SWATH TOFMS spectra of a Semtex sample on a glass slide with TOF/MS (top) and formula finder for PETN [M+NO3]⁻(Middle) and RDX [M+NO3]⁻ (bottom).